

A novel fluorinated europium ternary complex for highly efficient pure red electroluminescence

Xiao Li^a, Guoyong Xiao^a, Haijun Chi^a, Yan Dong^a, Hongbin Zhao^a, Peng Lei^a, Zhiqiang Zhang^a, Zhizhi Hu^a, Shuanghong Wu^b, Zisheng Su^b, Wenlian Li^{b,*}

^a School of Chemical Engineering, University of Science and Technology Liaoning, Anshan 114051, People's Republic of China

^b Key Laboratory of Excited State Processes, Changchun Institute of Optics, Fine Mechanics and Physics, Chinese Academy of Sciences, Changchun 130033, People's Republic of China

ARTICLE INFO

Article history:

Received 2 January 2010

Received in revised form 28 March 2010

Accepted 12 April 2010

Keywords:

Optical materials

Synthesis

Luminescence

Multilayers

ABSTRACT

A novel fluorine-functionalized europium(III) ternary complex, i.e., Eu(DBM)₃(BFPP), in which DBM was dibenzoylmethane and BFPP 2, 3-bis(4-fluorophenyl)pyrazino[2,3-*f*] [1,10]phenanthroline, was designed, synthesized and characterized. The complex emits the characteristic red emission of trivalent europium ion due to the ⁵D₀ → ⁷F_j (*j*=0–4) transitions under photo excitation with good luminescent quantum efficiency (0.55) and exhibits high thermal stability (387 °C). The organic light-emitting diodes (OLEDs) employing the complex as a dopant emitter with the structures of ITO/TPD (40 nm)/CBP:Eu-complex (30 nm)/Bphen (10 nm)/Alq₃ (20 nm)/LiF (1 nm)/Al (150 nm) were successfully fabricated. The 4 wt.% Eu(DBM)₃(BFPP) doped device exhibited the maximum luminance of 1766 cd/m² and a peak current efficiency of 4.6 cd/A, corresponding to the high external quantum efficiency of 2.27%.

© 2010 Elsevier B.V. All rights reserved.

1. Introduction

As one of the most promising next-generation low-cost, full-color and flat-panel displays, organic light-emitting diodes (OLEDs) have been intensively pursued and much progress has been achieved since the initial work by Tang [1] and Burroughes [2]. OLEDs with phosphorescent materials as the emitters can offer nearly 100% internal quantum efficiencies, so phosphorescent materials such as the heavy metal complexes of Ir(III) [3–5], Pt(II) [6], Re(I) [7–9], etc. have been much sought. Although highly efficient performances of the devices based on those phosphorescent materials as emitters have been achieved, it is especially difficult to obtain pure emission colors from them because their emission spectra usually have a full width at half maximum (FWHM) of 50–100 nm or even wider which are not well suitable for actual display applications. In contrast, luminescent lanthanide complexes are believed to be promising candidates to solve this problem because lanthanide complexes can generate extremely pure emission. Since the 4f shells of trivalent lanthanide ions are well shielded by the filled 5s and 5p orbitals, the 4f energy levels are only weakly perturbed by the environment outside the lanthanide ions. Furthermore, it is well known that lanthanide complexes are central-ions-luminescence phosphor materials in which trivalent lanthanide ions possess 4f

electron configuration, which are not only different from Alq₃ that is ligand-central fluorescent material but also Ir(III) complexes that their electroluminescence (EL) results from radiative relaxation from metal-to-ligand charge transfer (³MLCT) state to ground state. Therefore, modification of the ligand based on lanthanide complexes does not result in high emission wavelength shift. Lanthanide complexes have further advantages that their internal quantum efficiency can rise up to 100% theoretically because both singlet and triplet excitons can be harnessed in the emissive process. Of the lanthanide complexes studied, europium (III) (Eu(III)) complexes are the most attractive pure red light-emitting materials in OLEDs. Despite efforts of several groups to apply Eu(III) complexes as red emitters in OLEDs, only limited success has been achieved [10–12]. Recently, there are a few reports on the improved EL performances of the fluorine-functionalized Ir(III) complexes [13–15], but OLEDs that utilize fluorine-functionalized Eu(III) complexes as the emitters are less investigated [16–18].

Inspired by those works, we reported the synthesis and photophysical properties of a europium complex, i.e., Eu(DBM)₃(BFPP), in which DBM is dibenzoylmethane and BFPP 2, 3-bis(4-fluorophenyl)pyrazino[2,3-*f*] [1,10]phenanthroline, and the use of this complex as pure red emitter in OLEDs. DBM was chosen as the first ligand due to its relatively high photoluminescence (PL) efficiency in Eu(III) complexes. 1,10-phenanthroline is included as the second ligand since it can enhance the stability of the Eu(III) complexes in addition to saturating the coordination number of the Eu(III) complexes. Two fluorine-substituted phenyls were intro-

* Corresponding author. Tel.: +86 431 86176345; fax: +86 431 86176345.

E-mail address: wllioled@yahoo.cn (W. Li).

duced through rotary σ bonds for not only improving PL efficiency, volatility for thin film deposition, enhancing electron mobility of the compounds and so on [18–20], but also providing bulky space effect resulting in suppressing the molecular aggregation and concentration quenching. Therefore, $\text{Eu}(\text{DBM})_3(\text{BFPP})$ is expected to exhibit the combined properties, thus leading to highly efficient pure red EL. As a result, a peak luminance of 1766 cd/m^2 and a maximum current efficiency of 4.6 cd/A , corresponding to the external quantum efficiency of 2.27% were achieved in the OLEDs using $\text{Eu}(\text{DBM})_3(\text{BFPP})$ as a dopant in the host of 4,4'-N,N'-dicarbazolebiphenyl (CBP).

2. Experimental

2.1. Reagents and physical measurements

Commercially available reagents and starting materials were used for synthesis of $\text{Eu}(\text{DBM})_3(\text{BFPP})$. Solvents were purified and dried by standard procedures prior to use. ^1H NMR spectra were recorded on a Bruker AC 500 spectrometer with tetramethylsilane (TMS) as an internal reference. Mass spectroscopy (MS) was performed on an Agilent 1100 LC/MSD Trap VL spectrometer. Elemental analysis was performed on Vario EL III CHNS instrument. Infrared spectrum was recorded with samples as KBr pellets using WQF 200 FTIR spectrophotometer. Thermogravimetric analysis (TGA) was performed on a PerkinElmer Diamond TG-DTA 6300 thermal analyzer. UV–vis absorption spectrum was obtained on a PerkinElmer Lambda 900 spectrophotometer. PL spectra were measured on a PerkinElmer LS 55 fluorescence spectrophotometer. The luminescent lifetime of $\text{Eu}(\text{DBM})_3(\text{BFPP})$ in solid state was detected by a system equipped with a TDS 3052 digital phosphor oscilloscope pulsed Nd:YAG laser with a Third-Harmonic-Generator (THG) 355 nm output.

2.2. Synthesis of $\text{Eu}(\text{DBM})_3(\text{BFPP})$

2.2.1. Synthesis of 1,10-phenanthroline-5,6-diamine

1,10-Phenanthroline-5,6-diamine was synthesized according to generally modified procedures [21,22]. Yield: 52%. ^1H NMR (DMSO , TMS): 8.827 (t, $J = 2.57 \text{ Hz}$, 2H), 7.785 (t, $J = 4.32 \text{ Hz}$, 2H), 6.225 (s, 4H).

2.2.2. Synthesis of BFPP

1,10-Phenanthroline-5,6-diamine (1.05 g, 5.0 mmol) and 1,2-bis(4-fluorophenyl) ethane-1,2-dione (1.48 g, 6.0 mmol) were refluxed in 25 mL of glacial acetic acid for 4 h under nitrogen atmosphere. The mixture was cooled to room temperature (RT) and filtered. The resulting solid was washed by ammonia and water and recrystallized by methanol to obtain light white solid powders. Yield: 85%. ^1H NMR (CDCl_3 , TMS): 7.336–7.653 (m, 6H), 7.691 (d, $J = 7.69 \text{ Hz}$, 4H), 8.575 (d, $J = 3.98 \text{ Hz}$, 2H), 8.975 (d, $J = 7.86 \text{ Hz}$, 2H); MS (APCI): m/z 420.98 $[\text{M} + \text{H}^+]$.

2.2.3. Synthesis of $\text{Eu}(\text{DBM})_3(\text{BFPP})$

A solution of DBM (0.269 g, 1.2 mmol) and BFPP (0.168 g, 0.4 mmol) was dissolved in a mixture of hot ethanol under stirring. The solution turned pale immediately after sodium hydroxide (1.2 mL, 1 M) was added. Then $\text{EuCl}_3 \cdot 6\text{H}_2\text{O}$ (0.147 g, 0.4 mmol) was dissolved in ethanol and added dropwise to the stirred solution. The mixture was stirred at 60°C for 3 h. The white product was collected by filtration and recrystallized from ethanol with the yield of 62%. Elemental analysis for $\text{C}_{71}\text{H}_{47}\text{EuF}_2\text{N}_4\text{O}_6$. Calcd: C 68.65, H 3.81, N 4.51; Found: C 68.72, H 3.73, N 4.53. IR (KBr, cm^{-1}): 1599 ($-\text{C}=\text{O}$), 520 (Eu–N), 423 (Eu–O).

2.3. Fabrication and EL measurements of OLEDs

The devices were grown onto a pre-cleaned indium tin oxide (ITO) coated glass substrates with a sheet resistance of $25 \Omega \text{ sq}^{-1}$. The ITO-coated substrates were routinely cleaned by ultrasonic treatment in solvents and then cleaned by exposure to a UV-ozone ambient. All organic layers were deposited in succession without breaking vacuum ($3 \times 10^{-4} \text{ Pa}$). The devices were prepared with the following structures of ITO/TPD (40 nm)/CBP:Eu-complex (30 nm)/Bphen (10 nm)/Alq₃ (20 nm)/LiF (1 nm)/Al (150 nm), in which TPD (*N,N'*-diphenyl-*N,N'*-bis(3-methylphenyl)-1,1'-biphenyl-4,4'-diamine), Bphen (4,7-diphenyl-1,10-phenanthroline), and Alq₃ (tris(8-hydroxyquinoline)aluminum) were used as hole transporting layer, exciton blocking layer and electron transporting layer, respectively, and LiF/Al as the composite cathode. Deposition rates and thicknesses of the layers were monitored in situ using oscillating quartz monitors. Thermal deposition rates for organic materials, LiF, and Al were ~ 1 , ~ 1 , and $\sim 10 \text{ \AA/s}$, respectively. The emitting area of the device was defined as 10 mm^2 by cathode mask. EL spectra were measured with a Hitachi MPF-4 fluorescence spectrophotometer. The luminance–current–voltage (L – I – V) characteristics were measured with a 3645 DC power supply combined with a spot photometer and were recorded simultaneously with measurements. All measurements were carried out at RT under ambient conditions.

3. Results and discussion

3.1. Synthesis, characterization and thermal stability of $\text{Eu}(\text{DBM})_3(\text{BFPP})$

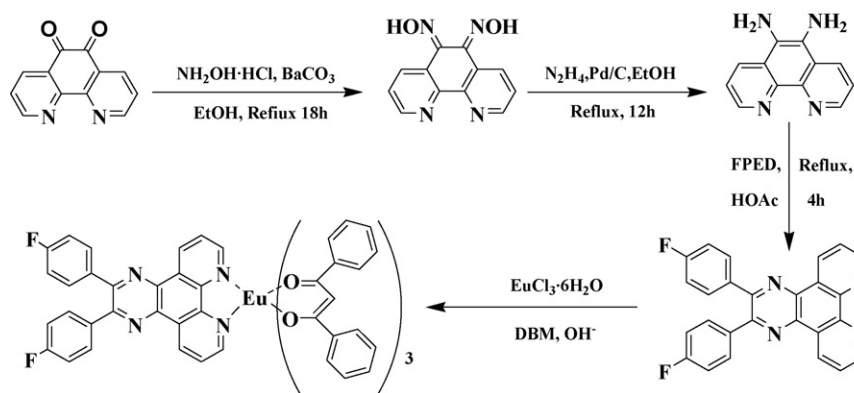
The synthetic pathways of $\text{Eu}(\text{DBM})_3(\text{BFPP})$ are outlined as shown in Scheme 1. BFPP was synthesized by a serial of reaction such as oxidation, condensation, catalytic reduction and so on and confirmed by ^1H NMR and MS. This complex was obtained from $\text{EuCl}_3 \cdot 6\text{H}_2\text{O}$, BFPP and DBM in the hot ethanol with the yield of 62%. The elemental analysis data for the complex are in good agreement with the calculated values. In the IR spectrum of $\text{Eu}(\text{DBM})_3(\text{BFPP})$, there are typical vibrations at $\sim 1599 \text{ cm}^{-1}$ for DBM[−] ligand coordinated Eu(III) central ion. The weak absorption bands at 520 and 423 cm^{-1} were ascribed to Eu–N and Eu–O vibrations, respectively. All evidences indicate that DBM[−] and BFPP coordinate to the central Eu(III) ion.

In order to investigate whether $\text{Eu}(\text{DBM})_3(\text{BFPP})$ is suitable for fabricating EL devices by vacuum deposition method, the decomposition temperature is determined from the TGA curve of the complex measured under nitrogen stream. The decomposition temperature of this complex is as high as 387°C , indicating that this complex exhibits high thermal stability and is favorable to fabrication of OLEDs by vacuum deposition.

3.2. Optical properties

The UV–vis absorption spectrum of $\text{Eu}(\text{DBM})_3(\text{BFPP})$ in CH_2Cl_2 , and PL spectrum of $\text{Eu}(\text{DBM})_3(\text{BFPP})$ powder are shown in Fig. 1. The intense absorption bands located at around 350 nm for the Eu(III) complex, which match that of the free DBM, are associated with the π – π^* transition of DBM ligand, indicating that the coordination of the Eu(III) ion does not significantly influence the energy of the singlet state of the β -diketone ligand and the β -diketone ligand contributes to the key absorption for the complex.

The sharp spectral bands of PL are the characteristic emissions of the Eu(III) ion. The main emission peak at 612 nm with FWHM of 6 nm corresponding to the $^5\text{D}_0 \rightarrow ^7\text{F}_2$ transition of Eu(III) ion



Scheme 1. Synthetic pathways of $\text{Eu}(\text{DBM})_3(\text{BFPP})$. FPED: 1,2-bis(4-fluorophenyl) ethane-1,2-dione; DBM: dibenzoylmethane.

accompanied by several weak peaks of various other $^5\text{D}_0 \rightarrow ^7\text{F}_j$ ($j=0-4$) transitions. No emission from the ligand was found. It has been known that the emission originates from the excitation of ligand followed by intersystem crossing from the singlet to the ligand triplet state; intramolecular energy transfer from the lowest excited triplet state of the ligand then leads to the excitation of the central $\text{Eu}(\text{III})$ ion. The result indicates that complete energy transfer from the ligand to the center $\text{Eu}(\text{III})$ ion occurs. The PL quantum yield of $\text{Eu}(\text{DBM})_3(\text{BFPP})$ measured in CH_2Cl_2 was 0.55 by using quinine sulfate as a reference which has a quantum yield of 0.546[23].

The lifetime measurement for the excited state of $\text{Eu}(\text{III})$ ion was recorded under the excitation at 355 nm at RT. The luminescence decay curve of $\text{Eu}(\text{III})$ ion related to the $^5\text{D}_0 \rightarrow ^7\text{F}_2$ emission in the $\text{Eu}(\text{DBM})_3(\text{BFPP})$ powder is plotted in Fig. 2. Luminescence decay follows the single exponential equation: $y = A_1 \times \exp(-x/t_1) + y_0$, where A_1 is the initial intensity of luminescence decay, t_1 the luminescence decay lifetime and y_0 the random noise. Depending on the specific surrounding of the $\text{Eu}(\text{III})$ ion, this lifetime is usually found to be in the range of 0.3–0.8 ms [24,25], but the lifetime of the $^5\text{D}_0$ emitting level for $\text{Eu}(\text{DBM})_3(\text{BFPP})$ is 0.26 ms which is shorter than that.

3.3. EL properties

In order to investigate EL performances of $\text{Eu}(\text{DBM})_3(\text{BFPP})$ as red emitter, multilayer OLEDs shown in Fig. 3 were fabricated. Doping levels of this complex in the host of CBP were varied from 2 wt.%

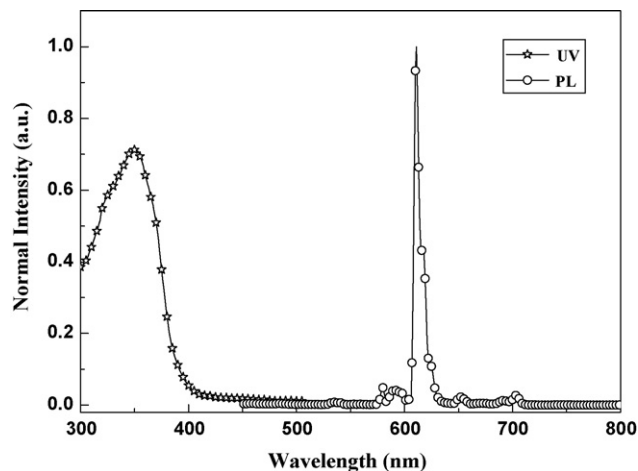


Fig. 1. UV-vis absorption spectrum of $\text{Eu}(\text{DBM})_3(\text{BFPP})$ in CH_2Cl_2 , and PL spectrum of $\text{Eu}(\text{DBM})_3(\text{BFPP})$ powder.

Table 1

EL performances of $\text{Eu}(\text{DBM})_3(\text{BFPP})$ doped devices with different ratios.

Ratio (wt.%)	V_{on}^a	η_{L}^b	L_{max}^c	λ_{max}^d
2	8.9	2.7	1148	612
4	7.8	4.6	1766	612
6	6.5	3.3	1700	612

^a Turn-on voltage (V).

^b Maximum current efficiency (cd/A).

^c Maximum luminance (cd/m²).

^d Maximum EL wavelength(nm).

to 6 wt.%. EL performances of the devices based on different ratios of $\text{Eu}(\text{DBM})_3(\text{BFPP})$ were summarized in Table 1. As shown in Table 1, the 4 wt.% $\text{Eu}(\text{DBM})_3(\text{BFPP})$ doped device exhibited the best performances. Fig. 4 shows the EL spectrum of 4 wt.% $\text{Eu}(\text{DBM})_3(\text{BFPP})$ doped device. It can be found that the EL spectrum with FWHM of 10 nm is almost identical to the PL spectrum, indicating that the EL emission at 612 nm originates from the $\text{Eu}(\text{III})$ ion. The emissive wavelength is independent of voltages from 8 V to 18 V.

Fig. 5 shows $L-I-V$ characteristics of 4 wt.% $\text{Eu}(\text{DBM})_3(\text{BFPP})$ doped device. It can be found that the luminance increases with increasing injection current as well as bias voltage in the device. The device exhibited the peak luminance of 1766 cd/m² at 14 V. The turn-on voltage was found to be ~8 V. The current efficiency-current density characteristic of the same device was also given in inset of Fig. 5. A maximum current efficiency of 4.6 cd/A was obtained at current density of 0.3 mA/cm², corresponding to the external quantum efficiency of 2.27%. When the current density increases to 100 mA/cm², the current efficiency is still as high as

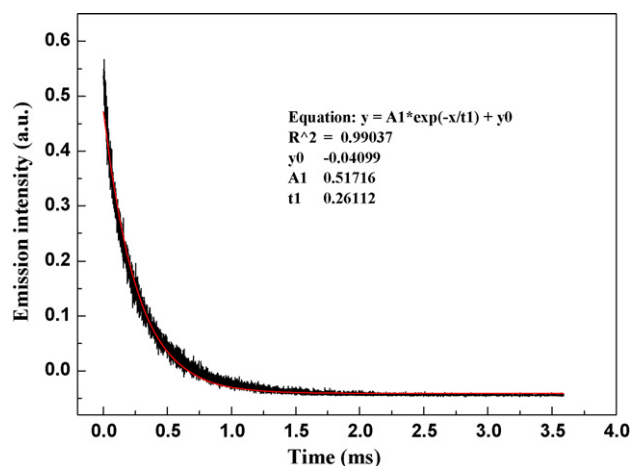


Fig. 2. Decay curve of $\text{Eu}(\text{III})$ excited state of $\text{Eu}(\text{DBM})_3(\text{BFPP})$.

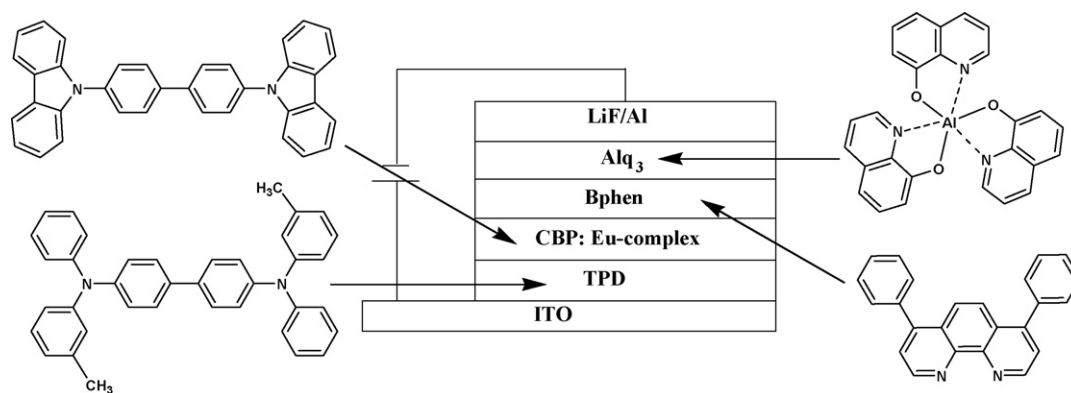


Fig. 3. The general structure of the devices and chemical structures of the compounds used in the devices.

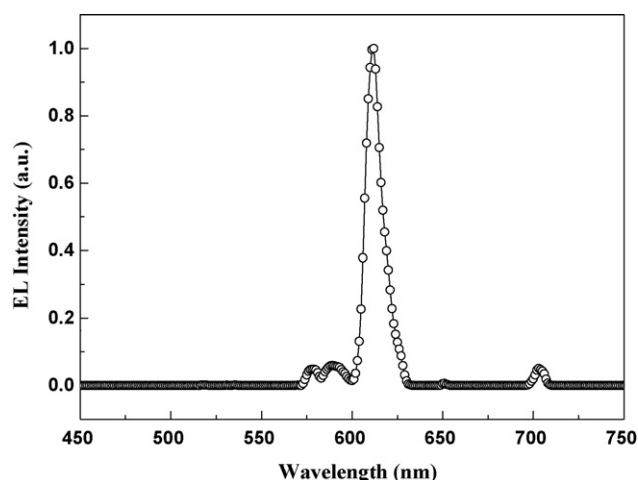


Fig. 4. EL spectrum of 4 wt.% $\text{Eu}(\text{DBM})_3(\text{BFPP})$ doped device at 16 V.

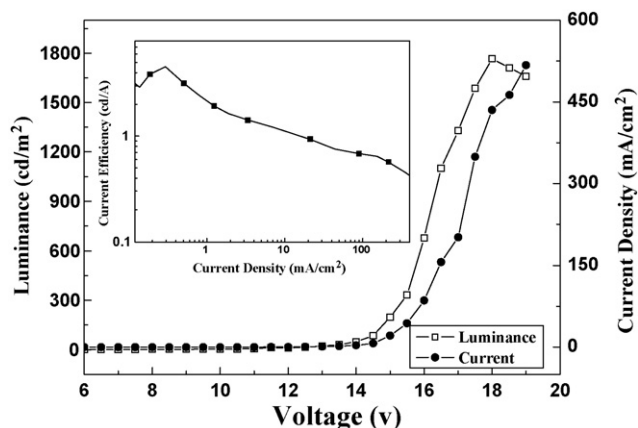


Fig. 5. L – I – V characteristics of 4 wt.% $\text{Eu}(\text{DBM})_3(\text{BFPP})$ doped device. Inset: Current efficiency–current density characteristic of the same device.

0.7 cd/A. These device performances are encouraging, compared to the representative EL devices based on the $\text{Eu}(\text{III})$ complexes so far reported [17,18]. The present results indicate that the introduction of fluorine into the Eu-complex is responsible for the outstanding device performances.

4. Conclusions

A novel europium(III) ternary complex with fluorine-functionalized substituents was designed, synthesized and characterized. Its photophysical properties were investigated in detail. The OLEDs based on $\text{Eu}(\text{DBM})_3(\text{BFPP})$ as a red dopant emitter exhibited encouraging results, demonstrating that such type complexes can be promising candidates for highly efficient pure red emission OLED applications. Future works on modifying the ligand's chemical structure and optimizing the device configurations would provide more satisfactory results.

References

- [1] C.W. Tang, S.A. VanSlyke, *Appl. Phys. Lett.* 51 (1987) 913.
- [2] M.A. Baldo, M.E. Thompson, S.R. Forrest, *Nature* 403 (2000) 750.
- [3] C.-F. Lin, W.-S. Huang, H.-H. Chou, J.T. Lin, *J. Organomet. Chem.* 694 (2009) 2757.
- [4] Y. You, S.Y. Park, *Dalton Trans.* (2009) 1267.
- [5] T.C. Lee, C.F. Chang, Y.C. Chiu, Y. Chi, T.Y. Chan, Y.M. Cheng, C.H. Lai, P.T. Chou, G.H. Lee, C.H. Chien, C.F. Shu, J. Leonhardt, *Chem. Asian J.* 4 (2009) 742.
- [6] C.-M. Che, C.-C. Kwok, S.-W. Lai, A.F. Rausch, W.J. Finkenzeller, N. Zhu, H. Yersin, *Chem. Eur. J.* 16 (2010) 233.
- [7] X. Li, D.Y. Zhang, W.L. Li, B. Chu, L.L. Han, J.Z. Zhu, Z.S. Su, D.F. Bi, D. Wang, D.F. Yang, Y.R. Chen, *Appl. Phys. Lett.* 92 (2008) 083302.
- [8] Z.J. Si, J. Li, B. Li, F.F. Zhao, S.Y. Liu, W.L. Li, *Inorg. Chem.* 46 (2007) 6155.
- [9] F. Li, M. Zhang, J. Feng, G. Cheng, Z.J. Wu, Y.G. Ma, S.Y. Liu, J.C. Shen, S.T. Lee, *Appl. Phys. Lett.* 83 (2003) 365.
- [10] P.-P. Sun, J.-P. Duan, H.-T. Shih, C.-H. Cheng, *Appl. Phys. Lett.* 81 (2002) 792.
- [11] M. Sun, H. Xin, K.-Z. Wang, Y.-A. Zhang, L.-P. Jin, C.-H. Huang, *Chem. Commun.* (2003) 702.
- [12] H.J. Tang, H. Tang, Z.G. Zhang, J.B. Yuan, C.J. Cong, K.L. Zhang, *Synth. Met.* 159 (2009) 72.
- [13] Y. Ha, J.-H. Seo, Y.K. Kim, *Synth. Met.* 158 (2008) 548.
- [14] G.Y. Xiao, P. Lei, H.J. Chi, Y.H. Lu, Y. Dong, Z.Z. Hu, Z.Q. Zhang, X. Li, *Synth. Met.* 159 (2009) 705.
- [15] C.-L. Ho, W.-Y. Wong, Q. Wang, D.G. Ma, L.X. Wang, Z.Y. Lin, *Adv. Funct. Mater.* 18 (2008) 928.
- [16] J.B. Yu, L. Zhou, H.J. Zhang, Y.X. Zheng, H.R. Li, R.P. Deng, Z.P. Peng, Z.F. Li, *Inorg. Chem.* 44 (2005) 1611.
- [17] L.Y. Zhang, B. Li, L.M. Zhang, P. Chen, S.Y. Liu, *J. Electrochem. Soc.* 156 (2009) 202.
- [18] Y.Y. Wang, L.H. Wang, X.H. Zhu, J. Ru, W. Huang, J.F. Fang, D.G. Ma, *Synth. Met.* 157 (2007) 165.
- [19] Y. Wang, N. Herron, V.V. Grushin, D. LeCloux, V. Petrov, *Appl. Phys. Lett.* 79 (2001) 449.
- [20] K.R. Justin Thomas, M. Velusamy, J.T. Lin, C.-H. Chien, Y.-T. Tao, Y.S. Wen, Y.-H. Hu, P.-T. Chou, *Inorg. Chem.* 44 (2005) 5677.
- [21] X.H. Zou, B.H. Ye, H. Li, J.G. Liu, Y. Xiong, L.N. Ji, *J. Chem. Soc. Dalton Trans.* (1999) 1423.
- [22] C. Abeywickrama, A.D. Baker, *J. Org. Chem.* 69 (2004) 7741.
- [23] K. Ye, J. Wang, H. Sun, Y. Liu, Z. Mu, F. Li, S. Jiang, J. Zhang, H. Zhang, Y. Wang, C.-M. Che, *J. Phys. Chem. B* 109 (2005) 8008.
- [24] F. Halverson, J.S.R. Brinen, J. Leto, *J. Chem. Phys.* 41 (1964) 157.
- [25] T.W. Canzler, J. Kido, *Org. Electron* 7 (2006) 29.